ESR investigations of platinum supported on alumina and titania

2 AUTHORS, INCLUDING:

Roel Prins
ETH Zurich
427 PUBLICATIONS **13,231** CITATIONS

Electron Spin Resonance Investigations of Platinum Supported on Al₂O₃ and TiO₂

Tom Huizinga* and Roel Prins

Laboratory for Inorganic Chemistry, Eindhoven University of Technology, 5600 MB Eindhoven, The Netherlands (Received: July 29, 1982; In Final Form: September 16, 1982)

Catalysts of Pt on Al₂O₃ and TiO₂ show various ESR signals. By measuring the effect of oxidation and reductions and by analyzing the *g* values and temperature dependencies we assigned two of the ESR signals to Pt^+ and Pt^{3+} ions. The Pt^+ signal is observed after reduction. Its fast relaxation demonstrates that it does not belong to isolated platinum cations but to Pt^+ ions in contact with platinum metal particles. These cations are situated at the metal–support interface. The Pt^{3+} signal is observed both after a direct oxidation as well as after a reduction and reoxidation treatment of the catalysts. Differences in shape and intensity of the signal show that after reoxidation the metal oxide crystallites are larger than after the primary oxidation.

Introduction

The interaction between the active component and the support is of great importance for the catalytic behavior of a heterogeneous catalyst. Thus the activity and selectivity of a supported metal catalyst may be altered by changing the nature of the support. For the conversion of synthesis gas it has been reported that when $Rh_4(CO)_{12}$ was impregnated on Al₂O₃ and SiO₂ and pyrolyzed to metallic rhodium the products were mainly hydrocarbons, whereas on La₂O₃, ZnO, and MgO oxygenated products were also formed.[1-3] Strong metal–support interactions are believed to explain the change in chemisorption behavior of TiO₂ supported metals (Pt, Ir, Rh) when they are reduced at high, instead of low, temperature,[4-6] although detailed explanations for this phenomenon are not yet available. Catalyst stability and resistance against sintering are also dependent on metal–support interactions. Much effort has been put into the study of the effect of variables such as temperature, pressure, and exposing gas on the sintering of supported metals and this resulted in two models for the sintering process, the atom and the crystallite migration model.[7,8]

In spite of the available information on various aspects of metal–support interactions, not much is known about the forces that play a role in the bonding of metal particles to a support on an atomic scale. For completely reduced metal particles (zero charge per metal atom) only van der Waals forces are possible, and these are weak on a per atom basis. Yet we know that for systems such as Pt/Al₂O₃ with an average metal particle size of 1.5 nm no sintering occurs in hydrogen up to 773 K.[9] If metal particles are not completely reduced, however, and if the metal ions in these particles are concentrated at the metal–support interface, then an ionic interaction with the oxygen anions of the oxidic support exists, which will be strong enough to explain good dispersion and high resistance for sintering. Metal ions have been proven to be present in macroscopic interfaces[10] between metals and oxidic materials. Also for Ni/SiO₂ catalysts it has been noticed that a good dispersion of nickel can only be obtained if the metal is not completely reduced.[11] Furthermore, from X-ray absorption studies of the Pt white lines of platinum catalysts it has been concluded that the platinum atoms in supported catalysts are, on the average, positively charged relative to the atoms in bulk platinum.[12-14]

The aim of this ESR investigation is to verify the idea that ions are present in reduced Pt/Al₂O₃ and Pt/TiO₂ systems.

Experimental Section

The alumina used was a high-purity η-Al₂O₃ with a surface area of 140 m² g⁻¹. The titania was made by hydrolysis of tetraethylorthotitanate. This resulted in a pure anatase with no iron contamination and a surface area of 90 m² g⁻¹. The platinum was deposited on the supports in the form of $Pt(NH_3)_4(OH)_2$ by using a combined ion exchange and wet impregnation method: A known amount of platinum salt was added to a well-stirred aqueous slurry of support at pH 9 and stirred for 6 h. Subsequently, the water was evaporated by slowly heating to 363 K. The metal content was 2 wt %.

In order to determine the metal particle diameters of the reduced samples, we applied X-ray diffraction, transmission electron microscopy, and hydrogen chemisorption. In XRD no metal peaks were observed, meaning that the average metal particle diameter is smaller than 4 nm. Particle diameters and distributions were obtained from TEM (see Figure 1) and hydrogen chemisorption. The total amounts of adsorbed hydrogen per metal atom (H/Pt) after reduction and evacuation at 573 K for 1 h were 1.3 and 0.7 for Pt/Al₂O₃ and Pt/TiO₂, respectively.

To measure ESR spectra in situ we used a reactor designed by Konings et al.[15] ESR spectra were recorded with a X-band Varian E-15 spectrometer equipped with a TE 104 dual sample cavity. The sample temperature was kept constant between 20 and 300 K with a Cryoson CE 5348 temperature controller. Signal intensity and position were

(1) Ichikawa, M. *Bull. Chem. Soc. Jpn.* **1978**, *51*, 2273.
(2) Ichikawa, M. *Bull. Chem. Soc. Jpn.* **1978**, *51*, 2268.
(3) Ichikawa, M. *J. Catal.* **1979**, *59*, 67.
(4) Baker, R. T. K.; Prestridge, E. B.; Garten, R. L. *J. Catal.* **1979**, *56*, 390.
(5) Horsley, J. A. *J. Am. Chem. Soc.* **1979**, *101*, 2870.
(6) Meriaudeau, P.; Ellestadt, H.; Naccache, C. 7th International Conference on Catalysis, Tokyo, 1980, p E-2.
(7) Ruckenstein, E. *J. Cryst. Growth* **1979**, *47*, 666.
(8) Chen, M.; Wang, T.; Schmidt, L. D. *J. Catal.* **1979**, *60*, 356.
(9) Dautzenberg, F. M.; Wolters, H. B. M. *J. Catal.* **1978**, *51*, 26.

(10) De Bruin, H. J.; Badwal, S. P. S.; Slattery, P. W. 4th CIMTEC, St. Vincent, Italy, 1979, p 1.
(11) Schats, W. M. T. M., Thesis, University of Nijmegen, 1981, p 57.
(12) Short, D. R.; Mansour, A.; Cook, Jr., J. W.; Sayers, D. E.; Katzer, J. R. *J. Catal.*, submitted for publication.
(13) Fukushima, T.; Katzer, J. R., 7th International Conference on Catalysis, Tokyo, 1980, p A-1.
(14) Lytle, F. W. *J. Catal.* **1976**, *43*, 376.
(15) Konings, A. J. A.; van Dooren, A. M.; Koningsberger, D. C.; de Beer, V. H. J.; Farragher, A. L.; Schuit, G. C. A. *J. Catal.* **1978**, *54*, 1.
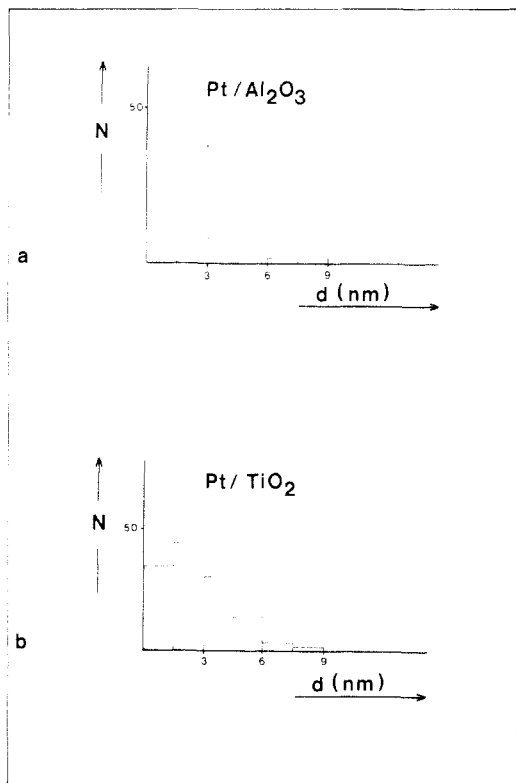
Figure 1. Particle size histograms as measured with electron microscopy: (a) Pt/Al_2O_3: $\bar{d}$ = 1.5 nm; (b) Pt/TiO_2; $\bar{d}$ = 3.1 nm.

calibrated with a Varian strong pitch sample (g = 2.0028, 3×10^{15} spins cm^{-1}). Both temperature and microwave power were varied to unravel the ESR spectra into their independent signals. All ESR spectra presented in the figures were recorded at 20 K. In the captions to figures the abbreviations used consist of a letter which indicates the pretreatment (I for impregnation, O for oxidation, R for reduction, and E for evacuation) and a number which is the temperature (in K) at which the pretreatment was carried out. All temperatures were reached with a heating rate of 5 K/min and were kept constant for 1 h.

Results and Discussion

Platinum is brought onto the support in the form of the Pt(NH_3)$_4$(OH)$_2$ complex. In this complex the platinum ion has the 2+ oxidation state and does not show an ESR signal. After oxidation at 623 K and purging with helium at 293 K a broad ESR signal appears (Figure 2a for Pt/Al_2O_3, Figure 2c for Pt/TiO_2). For Pt/Al_2O_3 the extrema and zero crossing are at g values of 2.64, 2.24, and 1.96. By doubly integrating the signal and comparing it with the Varian standard sample we calculate that this signal represents 3.5% of the total platinum amount. For Pt/TiO_2 we find extrema and zero crossing at 2.64, 2.26, and 2.00 and calculate that the signal represents 2.8% of the Pt atoms.

Oxidation at 623 K leads to the decomposition of the Pt^{2+} complex[16] and to the formation of platinum oxide like species, with a good spreading over the support surface. Since the most stable oxide of platinum is PtO_2[17] we presume that the majority of the platinum ions are in the 4+ oxidation state. When some of the small platinum species are not completely oxidized part of the platinum ions will be in the Pt^{3+} state. The g values of such a system
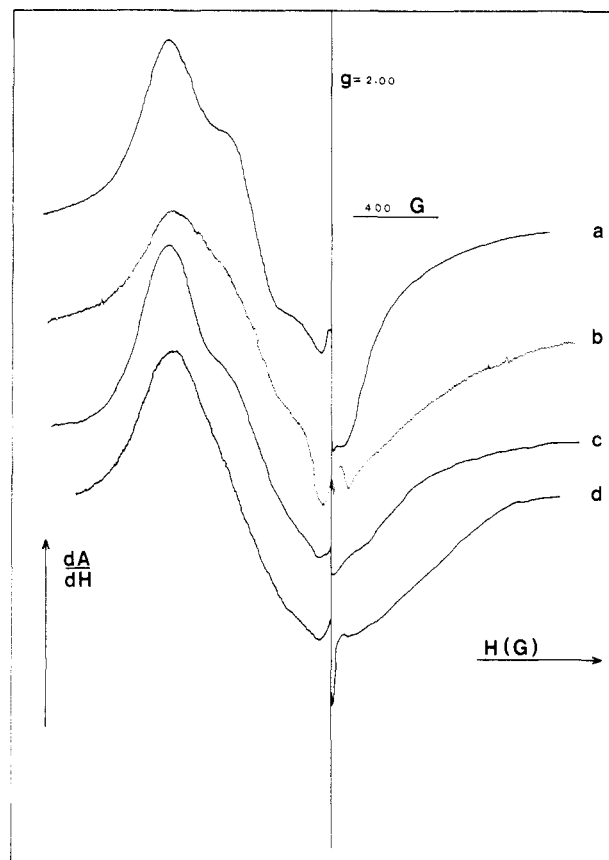

Figure 2. X-band ESR spectra of (a) Pt/Al_2O_3: O623, E273; (b) Pt/Al_2O_3: O623, R623, O623, E273; (c) Pt/TiO_2: O573, E273; (d) Pt/TiO_2: O573, R573, O573, E273.

(d^7, low spin, $S = 1/2$) will be above the g value of a free electron.[18] Therefore we assign the ESR spectrum to Pt^{3+} ions. The fact that $g_3 < 2.00$ for Pt/Al_2O_3 is due to second-order spin–orbit perturbation.[19]

Geschwind and Remeika (20) have observed for Pt doped single crystals of α-Al_2O_3 an ESR signal at g = 2.22 at 77 K, which they tentatively ascribed to Pt$^+$ ions, although they did not rule out Pt^{3+}. In their study of calcined Pt/Al_2O_3 catalysts Katzer et al.[21] observed a signal similar to our ESR signal and interpreted it as a signal with two g values and an isotropic hyperfine splitting, due to Pt^{3+} ions. Computer simulations make such an interpretation most unlikely. It proved impossible to simulate the experimental Pt^{3+} signal by varying the magnitude of the line width, the g-tensor components, and the hyperfine splitting component, while constraining the **g** tensor to axial symmetry. From these observations it is also clear that the experimental line widths are much too large to observe the relatively small hyperfine splitting of the Pt^{195} nucleus. The g values for Pt/TiO_2 are different from values published in the literature (g_1 = 2.33 g_2 = 2.15, g_3 = 1.95[22]), but in these studies other preparation methods were used.

Reduction of the oxidized Pt/Al_2O_3 sample at 623 K is expected to give metallic platinum. Although after such

(16) Shubochkin, L. K.; Gishchin, V. I.; Larin, G. M.; Kolosov, V. A. *Russ. J. Inorg. Chem.* **1974**, *19*, 249.

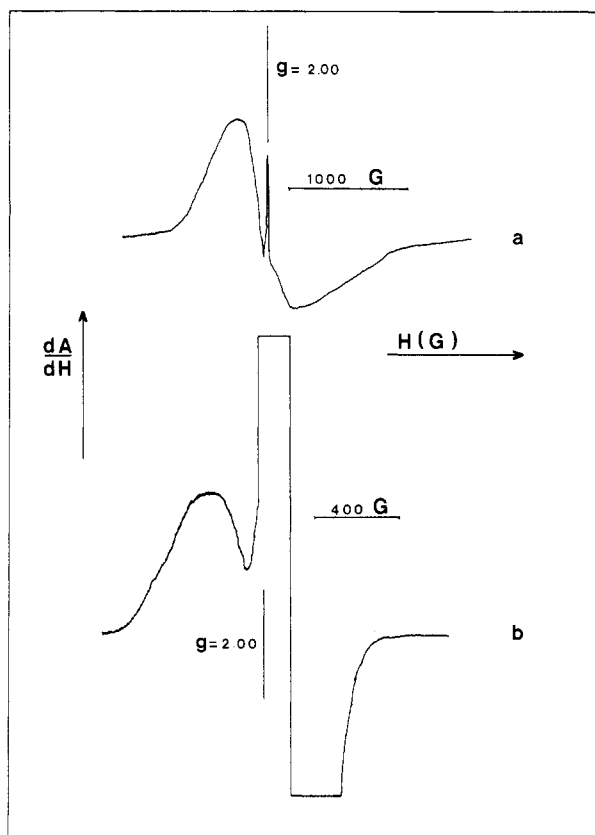(17) Chaston, J. C. *Platinum Met. Rev.* **1964**, *8*, 50.

(18) Wertz, J. E.; Bolton, J. R. "Electron Spin Resonance, Elementary Theory and Practical Applications"; McGraw-Hill: New York, 1972.

(19) Raizman, A.; Schoenberg, A.; Suss, J. T. *Phys. Rev. B* **1979**, *20*, 1863.

(20) Geschwind, S.; Remeika, J. P. *J. Appl. Phys. Suppl.* **1962**, *33*, 370.

(21) Katzer, J. R.; Schuit, G. C. A.; van Hooff, J. H. C. *J. Catal.* **1979**, *59*, 278.

(22) Chandrashekhar, G. V.; Title, R. S. *J. Electrochem. Soc.* **1976**, *123*, 392.

Figure 3. X-band ESR spectra of (a) Pt/Al₂O₃: O573, R573, E273; (b) Pt/TiO₂: O573, R573, E623.
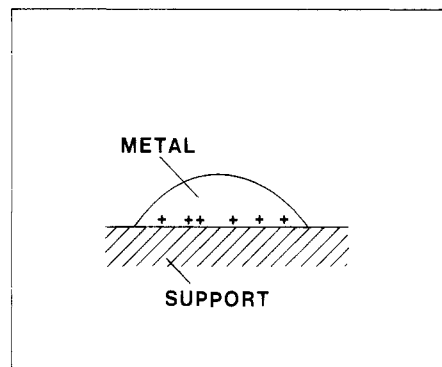

Figure 4. The metal–support interface.

coordinated by oxide anions, at the metal–support interface, since a position inside the metal particle or at the gas–metal interface is very unlikely.

About 0.4% of the total amount of platinum is in the Pt^+ state. Although this is only a minor amount, it still means that there are about two Pt^+ ions available per average platinum particle in the reduced catalyst ($\bar{d}$ = 1.5 nm). Taking into account that Pt^+ ions which are strongly magnetically coupled cannot be observed with ESR, nor can Pt^{2+} ions, we conclude that there are quite a few cations at the metal–support interface of these particles (Figure 4).

Reduction of the oxidized Pt/TiO₂ sample at 573 K leads to the appearance of a Ti^{3+} signal. In another publication[24] we have described the behavior of this signal. After reduction and evacuation at 573 K the Ti^{3+} signal is reduced in intensity and this allows us to see the left wing of a signal which centers around g = 2.0 and which has a line width of about 400 G (Figure 3b). Again this signal is not observable above 80 K. In concurrence with the Pt/Al₂O₃ case this signal is assigned to Pt^+ ions. The observations of ions in reduced systems is an important indication of the nature of the interaction between metal particles and the support. By leaving some atoms with a positive charge in the metal–support interface of the reduced particles there remains a Coulomb interaction between the metal and support.

Reoxidation of the Pt/Al₂O₃ samples leads to the reappearance of the Pt^{3+} signal (Figure 2b). Although the total span of the signal of the reoxidized sample is the same as after the initial oxidation, its line shape is now more symmetric. Furthermore, the intensity (0.8% of the platinum is Pt^{3+}) is smaller than after the initial oxidation (3.5%). Obviously, the environment of the Pt^{3+} ions is different from that after the first oxidation. After the primary oxidation the Pt^{3+} ions will be located on the Al₂O₃ surface as isolated ions, or may be as Pt^{3+} ions in small crystals of PtO₂. During reduction, migration and agglomeration of platinum atoms occurs and the average number of platinum atoms in the metal particles will be larger than that in the platinum oxide precursor particles. The average dimensions of the platinum particles formed for Pt/Al₂O₃ is 1.5 nm (cf. Figure 1) and a subsequent reoxidation will lead to PtO₂ particles of similar dimensions. The difference in environment of the Pt^{3+} ions explains the difference in shape of the ESR spectra, and the larger size of the platinum oxide crystals explains the smaller intensity.

Just like the Pt/Al₂O₃ sample, the Pt/TiO₂ sample showed a somewhat decreased Pt^{3+} signal intensity after reduction and reoxidation (1.5%). Again, the shape of the signal after reoxidation was more symmetric than after the

a treatment the Pt^{3+} signal had disappeared we do observe new ESR signals. Apart from a weak narrow signal at the free electron g value which will be neglected because of its weak intensity and its presence in the bare support, we observe an ESR signal at g = 2.05 and ΔH = 520 G (Figure 3a). The slightly positive deviation of g = 2.00 suggests that the signal comes from a d^9 system ($S = {}^1/_2$). Because of the occurrence of the signal both on Pt/Al₂O₃ and Pt/TiO₂ (see below), and not on the pure supports after the same treatments, we attribute this signal to Pt^+ (d^9, $S = {}^1/_2$). The temperature behavior of the signal intensity—at low temperatures according to Curie's law, deviations from this law between 60 and 80 K, and unobservable above 80 K—is unusual, however, for a d^9 system. Such a fast relaxation behavior has only been observed for d^9 metal ions with tetrahedral coordination and such platinum cations are very uncommon. For instance, tetrahedrally coordinated palladium cations have only been observed with specially designed ligands in organometallic complexes.[23] In our systems with oxide anions as ligands this will not be the case. This also rules out that the g = 2.05 signal could be due to a Pt^{2+} d^8 species, since for octahedrally coordinated $5d^8$ ions the ground state is a zero spin state.

For these reasons we conclude that the Pt^+ ions do not occur as isolated ions, only surrounded by oxide anions, but that they are in contact with other platinum atoms or ions. In this way the possibility is opened for a fast relaxation via spin–spin or spin–lattice relaxation. Temperature-programmed reduction studies from our laboratory showed a high degree of reduction for this Pt/Al₂O₃ system, which rules out the possibility that the Pt^+ ions are imbedded in a PtO environment. This only leaves the possibility of Pt^+ ions in contact with platinum atoms and

(23) Lott, A. L.; Rasmussen, P. G. *J. Am. Chem. Soc.* **1969**, *91*, 6502.

(24) Huizinga, T.; Prins, R. *J. Phys. Chem.* **1981**, *85*, 2156.

initial oxidation (Figure 2d).

Type II DM Lyotropic Nematics and Their Derived Cholesteric Forms

P. S. Covello, B. J. Forrest, M. E. Marcondes Helene, L. W. Reeves,* and M. Vist

Chemistry Department, University of Waterloo, Waterloo, Ontario N2L 3G1, Canada (Received: September 4, 1981; In Final Form: June 4, 1982)

Several new nematic type II DM and related cholesteric type II aqueous lyotropic mesophases have been prepared. The disk-bilayer micelles in the liquid crystals have been based on *n*-dodecanoyl alaninate, serinate, and valinate amphiphiles as the principal component. In balanced optically racemic mixtures the systems are nematic. The derived cholesteric phases are prepared by using unbalanced mixtures of the single-center optically active amphiphile. For a series of mesophases in which the composition is fixed but the optical isomer ratio varied, the inverse pitch length is found to be proportional to the mole fraction difference between L and D forms of the detergent. The pitch lengths are an order of magnitude longer than those found for thermotropic cholesterics and increasing the water content initially decreases the pitch. At high water contents there is a region where the pitch is independent of water content and finally there is a very small lengthening of the pitch. The influence of small amounts of optically active guests has been investigated. In one case, for 2-octanol, both D and L forms lengthen the pitch by the same amount. The lamellar phase, which is formed at lower water contents, shows no cooperative features of a helical structure. It is concluded that the cholesteric behavior arises because the planar disk micelles are slightly twisted into partial helices and the resultant packing of these micelles leads to the helical order of a cholesteric phase. Pitch lengths measured indicate that the visible reflection phenomenon of thermotropic cholesterics are unlikely in the aqueous lyotropic systems.

Introduction

Thermotropic cholesteric liquid crystals[1] have been described as nematic planes arranged in a parallel array with a unique director in each plane which rotates either clockwise or counterclockwise along a direction normal to these planes. Balanced mixtures of opposite enantiomers yield nematic phases.[1-3] The unit of the cholesteric structure is a chiral molecule, though the dissolution of chiral molecules, even in dilute solution in a nematic, also produces an induced cholesteric phase. The distance, perpendicular to the nematic planes, which produces a 2π rotation of the director is called the pitch *p* of the cholesteric. In the case of thermotropic liquid crystals the indivisible unit of the structure is a molecule and the dominant forces, which provide for the existence of liquid crystalline forms, are *intermolecular*. The most generally applicable theories which account for nematic and cholesteric forms include the assumption of anisotropic dispersion forces or intermolecular potentials.[4-7]

Aqueous lyotropic nematic and cholesteric liquid crystals owe their origin to a completely different, and often *divisible*, unit. The unit of these structures is a *micelle*, which contains thousands of individual molecules or ions, and which, for nematics, may be rodlike or disklike in form.[8] The characteristic properties of textures in the polarizing microscope,[9,10] low-angle X-ray diffraction patterns,[11,12] and the spontaneous alignment in magnetic fields[13] allow retention of the term nematic structure. The long-range orientational order is a consequence of anisotropic forces between large *micelles*, which, by changing chemical conditions, may grow in size and even change their symmetry.[8] In summary, the thermotropic cholesteric structure derives directly from the dissymmetry of the basic molecular units but aqueous lyotropic cholesteric systems[10,14] have an intervening level of superstructure.[11,15] The basic unit of the micelle is an optically active am-

(1) M. G. Friedel, *Ann. Phys.*, **18**, 273 (1922).
(2) F. Sackmann, S. Meiboom, and L. C. Snyder, *J. Am. Chem. Soc.*, **90**, 3567 (1968).
(3) F. Sackmann, S. Meiboom, and L. C. Snyder, *J. Am. Chem. Soc.*, **89**, 5981 (1967).
(4) W. Maier and A. Saupe *Z. Naturforsch.*, **139**, 564 (1958); **149**, 882 (1959); **159**, 287 (1960).
(5) G. R. Luckhurst in "The Molecular Physics of Liquid Crystals", G. R. Luckhurst and G. W. Gray, Ed., Academic Press, New York, 1979, Chapter 4, p 85.
(6) P. G. DeGennes, *Mol. Cryst. Liq. Cryst.*, **7**, 325 (1969); also in "The Physics of Liquid Crystals", Clarendon Press, Oxford, 1974.

(7) H. Schroder in "The Molecular Physics of Liquid Crystals", G. R. Luckhurst and G. W. Gray, Clarendon Press, Oxford, 1979, Ed., Chapter 5, p 121.
(8) B. J. Forrest and L. W. Reeves, *Chem. Rev.*, **81**, 1 (1981).
(9) K. Radley and A. Saupe, *Mol. Phys.*, **35**, 1405 (1978).
(10) L. J. Yu and A. Saupe, *J. Am. Chem. Soc.*, **102**, 4879 (1980).
(11) L. Q. do Amaral, C. Freire Pimentel, M. R. Tavares, and J. A. Vanin, *J. Chem. Phys.*, **71**, 2940 (1979).
(12) L. Q. do Amaral and M. R. Tavares, *Mol. Cryst. Liq. Cryst. Lett.*, **56**, 203 (1980).
(13) K. D. Lawson and T. J. Flautt, *J. Am. Chem. Soc.*, **89**, 5489 (1967).
(14) M. Acimis and L. W. Reeves, *Can. J. Chem.*, **58**, 1533 (1980).
(15) Y. Hendrikx and J. Charvolin, *J. Phys.*, **42**, 1427 (1981).